



Study of Ion Induced Pressure Instability in the ILC Positron Damping ring

O.B. Malyshev¹

September 30, 2008

Abstract

Ion induced pressure instability is a potential problem for the ILC positron damping ring (DR) if the chosen pumping scheme does not provide sufficient pumping. The ion induced pressure instability effect results from ionisation of residual gas molecules by the beam particles, their acceleration in the field of the beam towards the vacuum chamber walls, causing ion induced gas desorption from vacuum chamber walls; these gas molecules in their turn can also be ionised, accelerated and cause further gas desorption. If the pumping is insufficient, this effect may cause a pressure instability, in which the pressure in the beam chamber grows rapidly to an unacceptable level. To analyse the ion induced pressure instability in the ILC positron DR the energy gained by ions was calculated for the appropriate beam parameters; it was found that the energy gain of ions will be about 300 eV. The ion induced gas desorption was estimated, and pumping solutions to avoid the ion induced pressure instability are suggested. The cheapest and most efficient solution is to use NEG coated vacuum chamber.

1) ASTeC/CI, STFC Daresbury Laboratory, Warrington, UK

STUDY OF ION INDUCED PRESSURE INSTABILITY IN THE ILC POSITRON DAMPING RING*

O.B. Malyshev[#], AStEC/CI, STFC Daresbury Laboratory, Warrington, UK

Abstract

Ion induced pressure instability is a potential problem for the ILC positron damping ring (DR) if the chosen pumping scheme does not provide sufficient pumping. The ion induced pressure instability effect results from ionisation of residual gas molecules by the beam particles, their acceleration in the field of the beam towards the vacuum chamber walls, causing ion induced gas desorption from vacuum chamber walls; these gas molecules in their turn can also be ionised, accelerated and cause further gas desorption. If the pumping is insufficient, this effect may cause a pressure instability, in which the pressure in the beam chamber grows rapidly to an unacceptable level. To analyse the ion induced pressure instability in the ILC positron DR the energy gained by ions was calculated for the appropriate beam parameters; it was found that the energy gain of ions will be about 300 eV. The ion induced gas desorption was estimated, and pumping solutions to avoid the ion induced pressure instability are suggested. The cheapest and most efficient solution is to use NEG coated vacuum chamber.

1. INTRODUCTION

The ion induced pressure instability was firstly observed at CERN in 1973 as an effect limiting the beam current in the ISR [1-3]. This effect and its key parameters were intensively studied in the following years [1-8]. It was found that the ion induced pressure instability develops as follows: first the residual gas molecules in the beam vacuum chamber are ionised by the beam particles; when these ions are accelerated in the field of a positively charged bunch towards the vacuum chamber walls, they collide with the wall and induce gas desorption. The gas molecules thus produced can in turn also be ionised, accelerated and cause further gas desorption. If the pumping is insufficient, this effect may cause pressure instability, i.e. pressure in the beam chamber grows rapidly by some orders of magnitude. Later, this effect was also investigated for the SSC [9] and LHC [10-12] storage rings, and considered in the vacuum system design. The aim of the work reported here was to study

*Work supported by the Commission of the European Communities under the 6th Framework Programme "Structuring the European Research Area", contract number RIDS-011899.

[#]o.b.malyshev@dl.ac.uk

whether the ion induced pressure instability is a potential problem for the ILC positron damping ring.

2. MODEL

The beam-gas-surface interaction model was developed in earlier papers: the single gas model was used in references [1-3, 7] and the multi-gas model is described in detail in ref. [8] and briefly in ref. [9]. The latter considers that the ions of a generic gas species can desorb other gas species. Therefore, the equilibrium equations for the gas density of each species will be cross-correlated. Following [8], a system with N gas species, A_i ($i=1,2\dots N$), can be described with the following equations for the volumetric molecular density $n_i(z,t)$ of the species A_i :

$$V \frac{dn_i}{dt} = \eta_i \dot{\Gamma} + \sum_{j=1}^N \frac{\chi_{A_i, A_j^+} I \theta_{A_j}}{e} n_i - C_i n_i + u_i \frac{d^2 n_i}{dz^2}; \quad (1)$$

where the first term on the right hand side of equation (1) accounts for the photo-stimulated desorption; the second term accounts for the ion induced desorption from the vacuum chamber wall; the third term accounts for the distributed pumping along the wall; and the last term accounts for the axial molecular diffusion. It was assumed here that the parameters are constant in time and do not depend on the axial co-ordinate z . The notation is as follows: V is the vacuum chamber volume per unit axial length; η is the photo-desorption yield; $\dot{\Gamma}$ is the photon intensity per unit axial length; χ is the ion stimulated desorption yield; I is the positron beam current; e is the electron charge; θ is the ionisation cross section of the residual gas molecules for beam positrons; $C_i = \alpha_i S_i$ is the distributed pumping speed of the beam screen holes per unit axial length, α is the sticking probability, $S_i = A \bar{v}_i / 4$ is the ideal wall pumping speed per unit axial length, \bar{v} being the mean molecular velocity; $u_i = A_c D_i$ is the specific vacuum chamber conductance per unit axial length, A_c is the vacuum chamber cross section, and D is the Knudsen diffusion coefficient.

Solving the system of N equations in quasi-static conditions, where $V dn/dt \approx 0$ and $A ds/dt \neq 0$, for gas densities $n_i(z)$ one can find the gas density inside the vacuum chamber. For example, in a two-gas model the solution is in the form:

$$\begin{cases} n_1(z) = \frac{q_2 d_1 + c_2 q_1}{c_1 c_2 - d_1 d_2} + k_1 e^{\sqrt{\omega_1} z} + k_2 e^{-\sqrt{\omega_1} z} + k_3 e^{\sqrt{\omega_2} z} + k_4 e^{-\sqrt{\omega_2} z}; \\ n_2(z) = \frac{q_1 d_2 + c_1 q_2}{c_1 c_2 - d_1 d_2} + K_1 e^{\sqrt{\omega_1} z} + K_2 e^{-\sqrt{\omega_1} z} + K_3 e^{\sqrt{\omega_2} z} + K_4 e^{-\sqrt{\omega_2} z}; \end{cases} \quad (2)$$

where

$$\omega_{1,2} = \frac{1}{2} \left(\frac{c_1}{u_1} + \frac{c_2}{u_2} \pm \sqrt{\left(\frac{c_1}{u_1} - \frac{c_2}{u_2} \right)^2 + 4 \frac{d_1 d_2}{u_1 u_2}} \right);$$

with

$$\begin{aligned} q_1 = \eta_1 \Gamma; \quad c_1 = C_1 - \frac{\chi_{A_1, A_1^+} I \theta_{A_1}}{e}; \quad d_1 = \frac{\chi_{A_1, A_2^+} I \theta_{A_2}}{e}; \\ q_2 = \eta_2 \Gamma; \quad c_2 = C_2 - \frac{\chi_{A_2, A_2^+} I \theta_{A_2}}{e}; \quad d_2 = \frac{\chi_{A_2, A_1^+} I \theta_{A_1}}{e}. \end{aligned} \quad (3)$$

The constants k_j and K_j ($j=1..4$) are dependent on the conditions at the ends of vacuum chamber.

The gas densities n_1 and n_2 in equation (2) tend to infinity when the divisor $(c_1 c_2 - d_1 d_2)$ tends to zero. Hence the pressure stability criteria is $c_1 c_2 - d_1 d_2 > 0$ or

$$\left(C_1 - \frac{\chi_{A_1, A_1^+} I \theta_{A_1}}{e} \right) \left(C_2 - \frac{\chi_{A_2, A_2^+} I \theta_{A_2}}{e} \right) > \frac{\chi_{A_1, A_2^+} I \theta_{A_2}}{e} \frac{\chi_{A_2, A_1^+} I \theta_{A_1}}{e} \quad (4)$$

Solving this inequality for the beam current I one can find that the beam current must be below the so-called critical beam current, I_c , which is a solution for the equation $c_1 c_2 - d_1 d_2 = 0$. The vacuum will be stable as long as the beam current is lower than the critical current.

3. ION IMPACT ENERGY

One of the parameters for calculating the critical beam current is the ion induced desorption. The ion induced desorption was studied experimentally at CERN [4-8]. It was found that the ion induced desorption yields depend on the choice of the material and its cleaning and conditioning, and increases with the ion impact energy.

For the present case, the ion energy was estimated using a procedure described in previous studies [11]. The probability of ionisation $\rho(x,y)$ of the residual gas molecules is proportional to the density of positrons in the bunch at the molecule position (x,y) at the ionisation time. For a Gaussian distribution of particles in the beam:

$$\rho(x, y) \propto 2\pi r e^{-xy/(\sigma_x \sigma_y)}; \quad (5)$$

where σ_x and σ_y are the transverse rms beam sizes. The energy of ions hitting the beam vacuum chamber wall depends on the beam parameters and the initial ion position. Since $\sigma_x \gg \sigma_y$ for the ILC DR, the electric field, E_b , of the bunch in the ILC DR can be described with the Bassetti-Erskine formula (see e.g. [13]) adopted for flat beams [14] as follows:

$$E(x, y) = \frac{q_b}{4\pi\epsilon_0 l_b \sigma_x} \times \begin{cases} \sqrt{\frac{8}{\pi}} \cdot \frac{y\sigma_x}{x^2 + y^2} \left[1 - \frac{(y^2 - 3x^2)\sigma_x^2}{(x^2 + y^2)^2} \right] & \text{for } x, y > 3\sigma_x; \\ \text{otherwise:} \\ \exp\left[-\left(\frac{x-iy}{\sqrt{2}\sigma_x}\right)^2\right] \operatorname{erf}\left(\frac{y\frac{\sigma_x}{\sigma_y} + ix\frac{\sigma_y}{\sigma_x}}{\sqrt{2}\sigma_x}\right) - \exp\left[-\left(\frac{x+iy}{\sqrt{2}\sigma_x}\right)^2\right] \operatorname{erf}\left(\frac{y-ix}{\sqrt{2}\sigma_x}\right) + \\ + \exp\left[-\left(\frac{x+iy}{\sqrt{2}\sigma_x}\right)^2\right] \operatorname{erf}\left(\frac{y\frac{\sigma_x}{\sigma_y} - ix\frac{\sigma_y}{\sigma_x}}{\sqrt{2}\sigma_x}\right) - \exp\left[-\left(\frac{x-iy}{\sqrt{2}\sigma_x}\right)^2\right] \operatorname{erf}\left(\frac{y+ix}{\sqrt{2}\sigma_x}\right) \end{cases} \quad (6)$$

where q_b is the positron bunch charge, $\epsilon_0 = 8.85 \cdot 10^{-12}$ F/m is the permittivity of free space; c is the speed of light in vacuum; and l_b is the rms bunch length.

In the model for calculation of the ion energy, a newly created ion is accelerated by the peak electric field during the bunch passage and then drifts with a constant velocity until the next bunch arrives. An estimate of its final velocity can be obtained by numerical integration. The iteration formulae for the ion velocity and the radial position $r = \sqrt{x^2 + y^2}$ in the presence of a bunch are:

$$\begin{cases} v_n = v_{n-1} + E_b \frac{q}{m} \cdot \Delta t; \\ r_n = r_{n-1} + v_n \cdot \Delta t; \end{cases} \quad (7)$$

where $\Delta t = \tau / N$ is the time interval, $n = 1, 2, \dots, N$. The time interval should be chosen small enough so as not to influence the final result. This requirement was found to be satisfied for $N = 1000$. Between two bunches the ion drifts with velocity $v_d = v_N$ to the radial position r_d when a new bunch arrives: $r_d = r_N + v_N (T - \tau)$.

The results of the calculation of the ion energy are shown in Table 1 for arcs, long straights and wigglers. For each set of beam parameters, the ion energy was calculated for different initial positions of the ion across and along the beam, according the distribution of positrons within the bunch. The calculations were performed for H_2^+ , CO^+ , and CO_2^+ : no difference was found between them. The ion energy varies between 220 eV for largest σ_x and σ_y and 340 eV for smallest σ_x and σ_y in ILC DR. It was also found that variation of the bunch length between 6 mm and 9 mm does not affect the result.

Table 1. Ion energy calculated for different beam sizes.

		Arc	Straight	Wiggler
σ_x (m)	max	$1.3 \cdot 10^{-3}$	$1.3 \cdot 10^{-3}$	$2.7 \cdot 10^{-3}$
	min	$6.5 \cdot 10^{-4}$	$2.7 \cdot 10^{-4}$	$1.9 \cdot 10^{-4}$
σ_y (m)	max	$8.9 \cdot 10^{-6}$	$1.0 \cdot 10^{-5}$	$5.5 \cdot 10^{-6}$
	min	$5.6 \cdot 10^{-6}$	$5.6 \cdot 10^{-6}$	$3.8 \cdot 10^{-6}$
E (eV)	max	265	320	340
	min	220	220	320

4. INPUT DATA FOR SIMULATIONS

Ion stimulated desorption yields are key parameters for vacuum stability estimates. The ion stimulated desorption yield depends on the ion mass, ion energy and the surface conditions. There is a lack of experimental data. Some measurements have been made, mainly at CERN [4–8], but the results are not directly applicable as the measurements were made for higher energies and not for all necessary ion species. Therefore, the ion stimulated desorption yields shown in Table 2 were extrapolated from the existing experimental data following the procedure described in ref. [10].

Unfortunately there are no data available for the ion stimulated desorption yield from NEG coated surfaces at the same conditions. However, there are experimental data for photon stimulated desorption; these data demonstrated that the desorption yields from NEG coated stainless steel vacuum chamber (activated 180°C) is two order of magnitude lower than for an uncoated surface baked at 300°C [15]. Although the ion stimulated processes might differ from photon stimulated ones, it is still reasonable to expect that ion stimulated desorption yields from the NEG coated surface are lower than from uncoated surfaces. Therefore, using

the data for uncoated stainless steel, one can study the “worst case” scenario for the NEG coated chamber, i.e. the real NEG coated vacuum chamber should behave better.

Table 2. Ion stimulated desorption yields calculated for 300-eV ions.

Impact ion	χ , (molecules/ion)			
	H ₂	CH ₄	CO	CO ₂
316LN stainless steel				
H ₂ ⁺	0.07	0.005	0.05	0.007
CH ₄ ⁺	0.43	0.04	0.45	0.067
CO ⁺	0.64	0.06	0.80	0.12
CO ₂ ⁺	0.77	0.08	1.12	0.17
Pure aluminium				
H ₂ ⁺	0.18	0.008	0.07	0.022
CH ₄ ⁺	1.1	0.056	0.67	0.20
CO ⁺	1.6	0.088	1.2	0.36
CO ₂ ⁺	1.9	0.114	1.7	0.50
Ti alloy				
H ₂ ⁺	0.13	0.002	0.04	0.007
CH ₄ ⁺	0.80	0.015	0.38	0.067
CO ⁺	1.2	0.024	0.68	0.12
CO ₂ ⁺	1.4	0.031	0.95	0.17

5. RESULTS FROM CALCULATIONS OF PRESSURE STABILITY CRITERIA

The pressure instability was studied for the vacuum chamber as recommended in reference [16]: this consists of a round tube vacuum chamber with inner diameter (ID) 50 mm and a distance between pumps of 6 m for conventional vacuum chamber, or 40 m for NEG coated vacuum chamber. The results are shown in Table 3 and in Fig. 1. The pressure evolution as a function of the beam current is shown in Fig. 1 for both positron and electron damping rings for the 316LN stainless steel vacuum chamber. The pressure in the electron damping ring increases linearly with the beam current because of photon stimulated desorption. The pressure in the positron damping ring increases more quickly as the ion induced desorption becomes the main source of gas when the beam current excess 0.2 A.

The critical current calculated for different vacuum chamber materials and distances between UHV pumps is compared to the maximum design beam current $I_{\max} = 0.4$ A in Table 2. Taking into consideration that the ion stimulated desorption yields may vary significantly depending on cleaning treatment, bakeout procedure, duration of pumping, photon and electron bombardment, etc., it is reasonable to assume that the critical current is calculated with an accuracy of +100% / -50%. Therefore the pressure could be unstable if $I_c / I_{\max} < 2$.

One can see that if the distance between the UHV pumps ($S=200$ l/s) is 6 m [16], then the pressure is unstable in an aluminium vacuum chamber, and has a very small safety factor in the 316LN stainless steel and titanium vacuum chambers. If the distance between the UHV pumps ($S=200$ l/s) is 10 m then pressure is unstable for all three materials. This demonstrates that the critical current is larger for vacuum chambers with shorter distance between pumps.

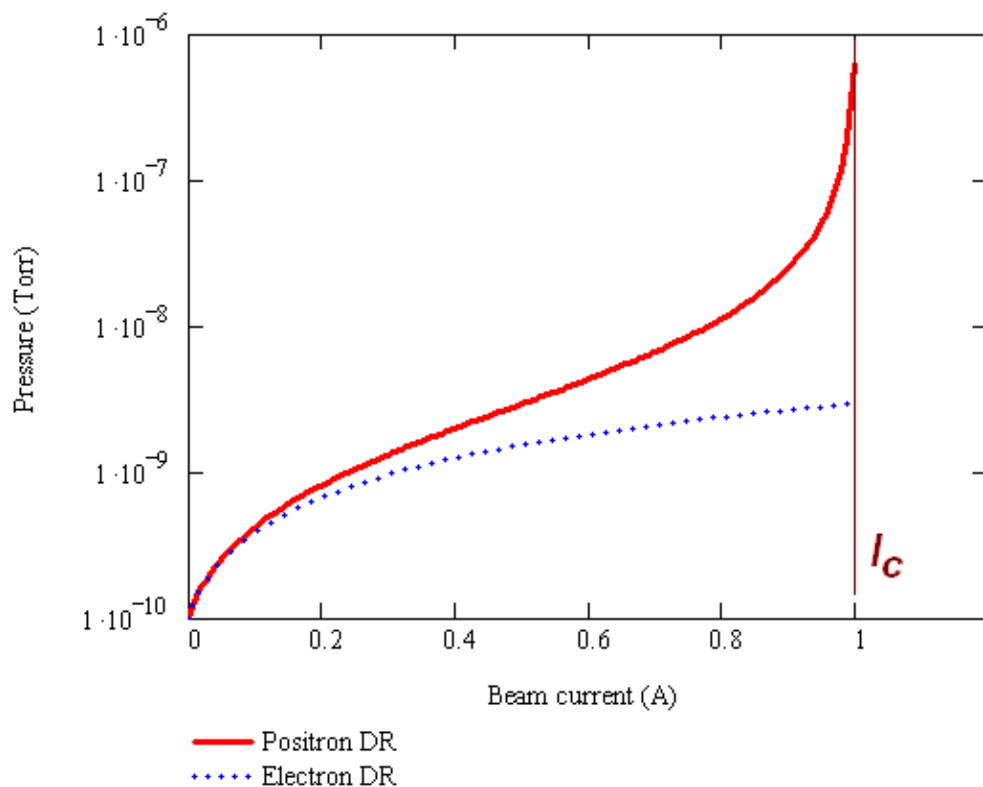


Figure 1. Pressure evolution as a function of the beam current for positron and electron damping rings for the 316LN stainless steel vacuum chamber.

The same calculations were performed for a vacuum chamber with larger diameter of vacuum chamber, ID = 60 mm, and 6 m distance between the pumps. This helps to increase the critical current by 20-25% which is still insufficient to allow the use of aluminium.

Finally, if a vacuum chamber made of aluminium, 316LN stainless steel or other material is coated with NEG (TiZrV) and the distance between the UHV pumps ($S=20$ l/s) is 40 m [16], then there is no pressure instability with a good safety margin: $I_c/I_{\max} = 12.5$. This technical solution allows much greater flexibility in the choice of material for vacuum chamber, diameter or cross section of vacuum chamber and distance between pumps.

Table 3. Ion stability of the ILC positron DR for different vacuum chamber materials ($I_{\max}=0.4$ A).

Vacuum chamber	I_c , (A)	I_c/I_{\max}	Dominant gas species	Stable or not
Distance between pumps L = 6 m, ID = 50 mm				
316LN	1.0	2.5	CO	Yes
Pure Al	0.5	1.25	CO	No
Ti alloy	1.1	2.8	CO	Yes
Distance between pumps L = 6 m, ID = 60 mm				
316LN	1.24	3.1	CO	Yes
Pure Al	0.64	1.6	CO	No
Ti alloy	1.4	3.5	CO	Yes
Distance between pumps L = 10 m, ID = 50 mm				
316LN	0.47	1.2	CO	No
Pure Al	0.24	0.6	CO	No
Ti alloy	0.53	1.3	CO	No
Distance between pumps L = 40 m, ID = 50 mm				
NEG coated	5	12.5	CH ₄	Yes

It is also important to mention the gas partial pressure pattern. In a baked accelerator vacuum chamber four gases are mainly presented: H₂, CO, CO₂ and CH₄. The gas spectrum changes when $I/I_c > 0.25$. Inside a stainless steel or aluminium vacuum chamber, molecules of

CO and CO₂ play a dominant role for the ion induced pressure (in)stability because of the lower effective pumping speed and higher ion stimulated desorption yield than for other gas species; in this case, CO becomes a dominant gas species. However, if the vacuum chamber is NEG coated, this introduces large distributed pumping speed for CO, CO₂ and H₂. This results in the change of the dominant gas species to lighter masses (CH₄ and H₂) as well as giving a much larger critical current.

6. CONCLUSIONS

In this paper, the analysis of vacuum stability against ion induced desorption in the ILC positron DR is presented. It is found that gas species ionized by the beam can be accelerated in the field of the beam to impact the vacuum chamber walls with energies about 300 eV. Because of the lack of experimental data, the gas desorption yields were estimated from experiments with higher ion energy. These results were used to model the pressure instability in ILC positron DR. It was found that the ion induced pressure instability is a potential threat to the positron DR if the pumping speed is insufficient. TiZrV NEG coating is the best solution to guarantee the vacuum stability. In this case, a distance of 40 m between UHV pumps (assuming an effective pumping speed of 20 l/s N₂ [16]) is found to be adequate.

REFERENCES

- [1] R.S. Calder. Ion induced gas desorption problems in the ISR. *Vacuum* 24(10), 1974, p. 437.
- [2] E. Fischer and K. Zankel. The stability of the residual gas density in the ISR in presence of high intensity proton beam. CERN-ISR-VA/73-52. November 1973.
- [3] O.Gröbner. The dynamic behavior of pressure bumps in the ISR. CERN/ISR-VA/76-25. 8th June 1976.
- [4] A.G. Mathewson. Ion induced desorption coefficients for titanium alloy, pure aluminum and stainless steel. CERN-ISR-VA/76-5 (1976).
- [5] M.-H. Achard, R. Calder and A. Mathewson. The effect of bakeout temperature on electron and ion induced gas desorption coefficients of some technological materials. *Vacuum* 29 (2), 1978, p. 53.
- [6] N. Hilleret. Variation of the ion induced desorption yield with temperature and the nature of incident ions. Proc. of 4th ICSS and 3d ECSS, Paris, France, September 1980 v. 2, pp. 1221–1224.

- [7] J.-C. Barnard, I. Bojko and N. Hilleret. Desorption of H₂ and CO₂ from Cu by H₂⁺ and Ar⁺ ion bombardment. LHC Project Note 44. CERN, April 1996.
- [8] M.P. Lozano. Ion induced yield measurements from copper and aluminium. *Vacuum* 67 (2002) 339-345.
- [9] W. Turner. Ion desorption stability in superconducting high energy physics proton colliders. *J.Vac. Sci.Technol. A*14(4), Jul/Aug 1996, pp. 2026-2038.
- [10] O. Malyshev and A. Rossi. Ion desorption stability in the LHC. *Vacuum Technical Note* 99-20, CERN, December 1999.
- [11] O. Malyshev. Ion desorption vacuum stability in the LHC (Muligas mode). *Proc. of EPAC-2000*, Vienna, 22–26 June, 1998, pp. 948–950.
- [12] O. Malyshev. The ion impact energy on the LHC vacuum chamber walls. *Proc. of EPAC-2000*, Vienna, 26–30 June, 2000, pp. 951–953.
- [13] *Handbook of Accelerator Physics and Engineering*. Edited by A.W. Chao and M. Tigner. World Scientific Publishing Co. Pte. Ltd, 1999, p. 128-129.
- [14] S. Tzenov. Private communication.
- [15] V.V. Anashin, I.R. Collins, R.V. Dostovalov, N.V. Fedorov, A.A. Krasnov, O.B. Malyshev and V.L. Ruzinov. Comparative study of photodesorption from TiZrV coated and uncoated stainless steel vacuum chambers. *Vacuum* 75 (2), July 2004, pp. 155-159.
- [16] O. B. Malyshev. *Vacuum Systems for the ILC DR - EuroTeV report-2006-094*. Nov. 2006.